Analysis of WRF Model Ensemble Forecast Skill for 80 m Winds over Iowa

Shannon L. Rabideau
Atmospheric Science Program
Iowa State University
Ames, IA 50010
srab@iastate.edu

Mentor: Dr. Gene Takle

ABSTRACT

Accurate wind speed forecasts are very important for the growing wind energy industry due to the relationship between speed and power. In this study, forecasted wind speeds were compared to observed tower wind speeds at a height of 80 m for a total of 32 cases. The observed data was provided by MidAmerican Energy Company from a meteorological tower within their Pomeroy, IA wind farm. Statistical analyses were performed to determine the bias, mean absolute error, and root mean squared error of seven different planetary boundary layer schemes and two different model initializations (GFS and NAM) for each hour of the 54 hour forecast period. Ensembles of the schemes were also created, analyzed, and compared to the individual schemes in order to test hypotheses relating to forecast skill as measured by mean absolute error. Results show that GFS initialization more accurately predicts wind speeds than NAM initialization. The ensemble mean and YSU scheme are the most accurate predictors of wind speed, while the QNSE scheme is the worst. In general, wind speeds are predicted most accurately during a high pressure regime and least accurately during the passage of a cold front.

1. Introduction

Within the last decade, wind power has come to the forefront as a potential source of renewable energy. If just 20% of the potential wind power could be captured, 100% of the world's energy demand could be satisfied (Archer et al. 2005). Iowa has a particular opportunity to seize on this source of energy. Using surface station and sounding data from the National Climatic Data Center (NCDC) and using the Least Square Extrapolation method, wind speeds and wind power potential were estimated across the globe. Iowa was shown to have an average power rating of class 3, which is generally suitable for wind power generation, with

even greater values in the northwestern part of the state (Archer et al. 2005).

With wind turbines increasing in height over the past few years, more data analysis is needed for these "tall towers" (80 m and above). While surface and low-level data may be extrapolated to these heights, there are often errors associated with the process. This is largely due to the decreasing effect of surface roughness and the increasing effect of lower atmospheric features such as the low level jet (LLJ) or circulation patterns. Elliot and Schwartz (2005) examined data from tall towers located in Kansas, Indiana, and Minnesota. They found that the greatest effect on the wind resource was produced by the strength of the nocturnal and southerly winds. They also found that these winds are the greatest influence on the 50 m to 100 m wind shear, to a greater degree than previous extrapolation studies had indicated.

Another study showed that circulation patterns, as represented by the north – south gradient of 500 hPa heights and to a lesser extent by the AO and Niño 3.4 SST indexes, have the greatest impact on wind speed variability, regardless of season. Mean monthly wind speeds were computed from hourly data from eleven 70 m tall towers in Minnesota for the period from 1995 to 2003 (Klink 2007). The north – south pressure gradient captured between 22% and 47% of the variability. The tall towers also showed a "high degree of spatial correlation", suggesting that data from one location can approximate nearby locations with similar characteristics.

Takle et al. (1978) studied the characteristics of wind and wind energy for four stations in Iowa. They found that the 1/7 power law reasonably well predicted periods with moderate to high wind speeds but was less successful with low speeds. The highest average wind power was calculated to be during the spring with winds from the WNW to NNW.

Recently, it was shown through observed data (two NCDC data sets containing land-based sites across the contiguous US) that surface wind speeds have declined through the 1973-2005 period, particularly over the eastern United States and in the Midwest (Pryor et. al. 2009). This trend was reproduced by the MM5 RCM nested within the NCEP-2 reanalysis. However, no clear consensus was found to indicate a link between this trend and inter-annual variability.

Since energy density varies as the cube of the wind speed, the ability to accurately forecast wind speeds can be very useful (Burton et al. 2001). It is also very important to push for more and more accurate forecasts due to the large variability of wind speeds both in space and time.

Investigations have been made into how well models can forecast surface wind speeds. One such study compared wind speeds from the Fifth-Generation Penn State/ NCAR Mesoscale Model (MM5) to observations from NCDC stations and the Computational and Information Systems Laboratory (CISL) archive (Andersen 2007). The model was found to have limited success, generally overestimating mean monthly wind speeds, especially in the fall and winter seasons. It also did not represent the diurnal cycle well, both overestimating the daily minimum and failing to capture the sharp increase in wind speeds in the observations. Climatological trends for the period 1979 to 2004 were also compared between the model and the observed. The model did not perform very well, most often having weaker trends than the observed speeds.

Buckley et al. (2004) compared model predictions with observed data at 4 m, 10 m, 18 m, and 36 m. Wind speeds from the Regional Atmospheric Modelling System (RAMS) were used to compare with speeds from National Weather Service (NWS) stations for the period April 1998 to March 2000. The mean absolute error and the standard deviation of the difference between the two speeds were the primary comparisons used. Overall, the model produced realistic predictions, with the ratio of the forecasted to observed wind speeds varying from 0.8 to 1.2. However, the model had some diffi-

culty forecasting the transition between daytime and nighttime conditions.

Zhang and Zheng (2004) studied how well surface wind speeds were reproduced in relation to surface temperatures by five different model planetary boundary layer (PBL) parameterization schemes. The scheme forecasts were compared to observations from NOAA's Technical Development Laboratory U.S. and Canada Surface Hourly Observations. They found that all schemes underestimated the wind speeds during the day, and three overestimated them at night. Of all the schemes, the Blackadar performed the best in reproducing the diurnal cycle.

With the moderate success of models in predicting surface wind speeds, the question is raised of how well they may do with higher heights. Few studies have been done that compare model forecasts to observed data at the level of tall towers, and most of those have been for offshore locations. More research is needed, especially using quality measurements that exist at that height (have not been extrapolated).

The purpose of this study is to see how well various schemes of the Weather Research and Forecasting Model (WRF) and the MM5 can predict wind speeds at 80 m. With data taken from an 80 m tower within a wind farm, an accurate assessment of the different schemes' forecasting ability can be made, and comparisons can also be made concerning the specific characteristics of those schemes. This study focuses on a site in Iowa, which has not been done previously, and the results may serve as a proxy for other locations in the state. This information may be very useful to wind energy companies for operational use. Wind directions were not included within this study. With the flat terrain in Iowa and wind turbines often set up to face various directions, they were deemed less important than wind speeds.

In this study, the hypothesis is tested that WRF can forecast wind speeds at 80 m with an average mean absolute error < 2.0 m s^{-1} for the forecast period 38-48hr (approximately 8am – 6pm on day 2 of the 54 hr forecast period) in all seasons with a confidence level of 95%.

2. Observations and Model Configuration

Observed 80 m wind speeds were provided by MidAmerican Energy Company (MEC) from a meteorology tower within their Pomeroy, IA wind farm. The tower is located on the central, far eastern side of the farm (Figure 1). Data was provided for a year-long period from 1 June 2008 to 1 June 2009 in 10 min increments. Hourly averages were then created within a Fortran program by averaging the six values starting 20 min before the hour and ending 30 min after the hour. This was done since the average time for each 10 min step was assigned to end of that period. This averaging excluded data deemed to be "bad". For instance, there were many stretches of 0.80 m s^{-1} wind speeds that were excluded since they seemed suspect and no knowledge of their reason for occurring was available from MEC.

Location of Pomeroy, IA Meteorological and Wind Towers

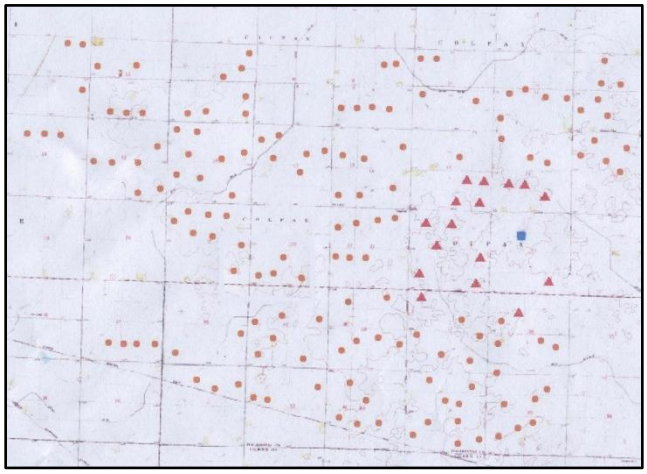

Figure 1: Location of meteorological tower (blue square) within Pomeroy, IA wind farm

Forecasted wind speeds were provided by a graduate student, Adam Deppe, and included a total of seven different schemes from two different forecasting models. The WRF and MM5

models produced 54-hr forecasts beginning at 00 UTC for a domain covering Iowa and surrounding states, with a grid resolution of 10 km (Figure 2). From the WRF, the MYJ, MYNN 2.5, MYNN 3.0, Pleim, QNSE, and YSU schemes were investigated (Table 1). From the MM5, the Blackadar scheme was investigated. Each of these schemes was also initialized with data from two different global models, the GFS and the NAM, creating a total of 14 different forecasts. The GFS and NAM ensemble means were also then computed within a program from each set of seven schemes to see if they might produce a more accurate forecast than the individual schemes.

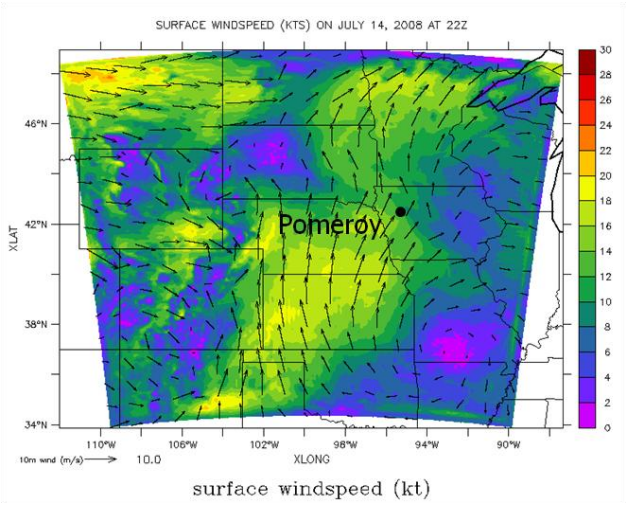

Figure 2: An example plot showing the location of the meteorological tower, the forecast domain, and the grid resolution.

3. Analyses

A number of statistical analyses were performed to quantify the accuracy of the forecasts and to show any tendencies exhibited by the individual schemes. A total of 32 cases were examined, with eight cases for each season in order to get a representative sample. For each case, a 54-hr forecast was produced, starting at 00 UTC, and compared to observations.

The hourly error was computed for each scheme forecast for each case.

$$Error = (f - o) \quad \text{(Eq. 1)}$$

Variable	Definition
f	forecasted wind speed
o	observed wind speed
X	sample set
x	sample value
n	sample size
μ	mean sample value

Table 2: Variable definitions for statistical analyses

The hourly normalized error was also computed for each scheme forecast for each case.

$$Normalized\ Error = (f - o)/o \quad \text{(Eq.2)}$$

The bias, mean absolute error (MAE), root mean squared error (RMSE), and standard deviation of the error were also computed. Each of these was computed for each forecast hour (calculated over all of the cases). Mean absolute error (MAE), with a confidence interval (CI) of 95%, was also computed for each season and over all cases.

$$Bias = \sum(f - o)/n \quad \text{(Eq. 3)}$$

$$MAE = \sum |(f - o)| / n \quad \text{(Eq. 4)}$$

$$RMSE = \sqrt{\sum(f - o)^2 / n} \quad \text{(Eq. 5)}$$

$$STDEV = \sqrt{\frac{\sum(x_{error} - \mu_{error})^2}{(n-1)}} \quad \text{(Eq. 6)}$$

$$CI = \mu \pm \left(\frac{STDEV\,(X)}{\sqrt{n}}\right) TINV(o.o5, n\text{-}1) \quad \text{(Eq. 7)}$$

These methods allow the accuracy and tendencies of the schemes to be shown as the forecast period progresses and also through different seasons or synoptic conditions.

The scheme performances were also compared by the synoptic conditions present through the forecast period. The conditions were determined using analyzed daily surface maps from

the Hydrometeorological Prediction Center (HPC). General comparisons were made based on the location of high and low pressure centers in relation to Pomeroy and any passage of warm or cold fronts during the period.

4. Results

a. Statistical analyses

The WRF can be a useful tool for forecasters when predicting the weather, but the initialization and planetary boundary layer scheme used can make a substantial difference in the accuracy of the forecast. Comparing the GFS against the NAM and the various PBL schemes against each other can help to determine the best individual scheme or combination forecast for different scenarios. Also, looking at one scheme from the MM5 (Blackadar), can show any significant differences between models.

When the mean absolute error of the forecasted speeds is plotted for each scheme, certain trends can be seen. First, comparing the GFS initialization (Fig. 3) to the NAM initialization (Fig. 4), it can be seen that both begin with a MAE around 1.5 m s^{-1} to 2.0 m s^{-1}, but about halfway through the period the NAM starts to have greater error than the GFS. For both initializations, the ensemble mean appears to have the lowest MAE, although the YSU also does fairly well. The QNSE has consistently higher MAE through the period. Another interesting feature is that the Blackadar does not do as well for the 12-22 hr forecast period, corresponding to daytime on the first full day of the forecast.

Some other interesting behavior can be seen by looking at the bias of each scheme throughout the forecast period (Figs. 5 and 6). There is not a large difference in the bias between the GFS initialization and the NAM initialization. However there are some very noticeable differences between the schemes. The YSU actually has the lowest average bias through the whole forecast period, with a bias 0.041 m s^{-1} lower than the ensemble for the GFS and 0.238 m s^{-1} lower than the ensemble for the NAM, though the bias is opposite in sign to the ensemble. The Blackadar scheme has a bias around twice as high as the other schemes, and it is shown to be consistently negative. The effect of the diurnal cycle of winds can also be clearly seen in the plots. The schemes as a whole have more trouble capturing the nighttime (6pm–6am LST) wind speeds, with an average bias of 0.460 m s^{-1}, than the daytime (6am–6pm LST) wind speeds, with an average bias of -0.032 m s^{-1}. The YSU does the best job of capturing the cycle with around a 2 m s^{-1} difference between the daytime and nighttime biases.

Examining the root mean squared error through the forecast period shows results similar to the mean absolute error. The NAM initialization (Fig. 7) again begins with a RMSE similar to the GFS initialization (Fig. 8), around 2 m s^{-1}, but increases through the period to end with a RMSE about 0.5 m s^{-1} to 1.0 m s^{-1} higher than the GFS. The ensembles again perform the best for both initializations; however for this analysis the MYNN 2.5 and MYNN 3.0 schemes have the highest RMSE, above the QNSE.

Looking at the standard deviation (Figs. 9 and 10), the general trend is what would be expected. The standard deviation increases the further out into time that the forecast goes, for both initializations. However, this increase is much greater in the NAM, ending over 1 m s^{-1} higher, compared to around 0.5 m s^{-1} for the GFS. It is interesting, though, that the Blackadar (MM5) scheme produces much less standard deviation with the NAM initialization through the second half of the forecast compared to the rest of the schemes (WRF schemes). Overall, the ensembles have the lowest average standard deviation, while the MYNN schemes have the largest.

Taking a closer look at the 38-48 hr forecast period (Tables 2 & 3) is useful for wind energy companies since this is the day 2 daytime period. Again, it can clearly be seen that the GFS has a lower MAE than the NAM (Figs. 11 & 12). On average, the GFS schemes have a MAE

of 1.696 m s^{-1} through the period, while the NAM schemes have a MAE of 2.294 m s^{-1}. Averaged over all of the cases, the WRF - GFS has a 95% confidence interval of 1.575 m s^{-1} to 1.817 m s^{-1}. The WRF - NAM has a 95% confidence interval of 2.149 m s^{-1} to 2.440 m s^{-1}. The only time that the GFS has a MAE (with 95% confidence) higher than 2 m s^{-1} is for hour 38, while the NAM is higher than the threshold throughout the period.

The ensemble mean has the lowest average MAE for the GFS at 1.529 m s^{-1}, as well as for

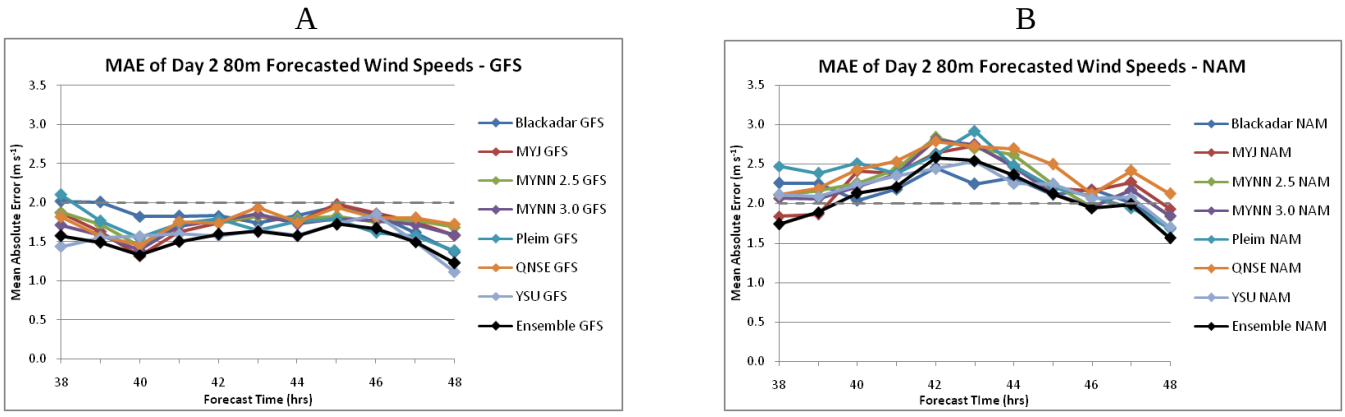

Figure 11: Mean absolute error of day 2 forecasts initialized by A) GFS and B) NAM during the daytime period

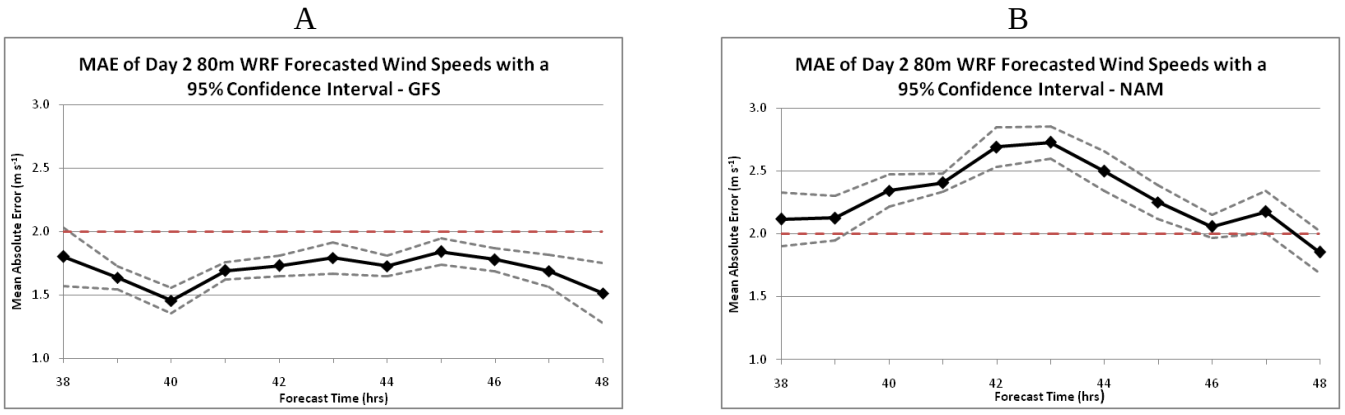

Figure 12: Average mean absolute error with a 95% confidence interval of day 2 forecasts initialized by A) GFS and B) NAM during the daytime period

the NAM with 2.098 m s^{-1}. The Blackadar performs the worst for the GFS (MAE = 1.806 m s^{-1}), while the QNSE performs the worst for the NAM (MAE = 2.421 m s^{-1}). Overall, it can again be clearly seen that the GFS has a lower MAE than the NAM.

Some interesting trends can also be seen by looking at the accuracy of the forecasts for each season (8 cases each). Both initializations perform significantly better in the spring than in other seasons (Table 4). The GFS has a fairly consistent MAE and confidence interval through the rest of the seasons. The NAM performs the worst in the fall, although the summer has a wide confidence interval with an upper bound comparable to the fall. One possible reason for the higher error in the summer could be that the models have difficulty forecasting the very low wind speeds that can occur through the season. However, another possibility is that there could

be some error in these findings since the summer cases had some data missing. The spring was the only season without a single missing forecast hour for the 8 cases.

Overall, the ensembles and the YSU have the lowest average mean absolute errors through all seasons except spring, where the MYNN schemes both perform well (Figure 13). The MYNN schemes tend to have some of the highest errors through the other seasons, though. On average, the Blackadar and QNSE perform the worst for each season.

b. Synoptic conditions

One way of possibly explaining the errors in the forecasts is to examine the synoptic conditions occurring during the cases and how the schemes have attempted to realize them. Cases were primarily organized by cold front passage, warm front passage, within high pressure, within low pressure, and in a transition area between high and low pressures. In general, cases with high pressure in the area around the wind farm had the lowest MAE, while cases with fronts passing over the area through the forecast period had the highest MAE (Figure 14). Cold fronts produced greater error than warm fronts on average. Transition areas occasionally produced high error, but it depended on the distance between the high pressure center and low pressure center. The stronger the pressure gradient, the stronger the winds, which may make forecasting more difficult for the models.

On average, the GFS produced less error than the NAM during the passing of fronts, and both were comparably accurate during high pressure. There were not enough cases of low pressure to draw any conclusions for that condition. For the schemes, the ensemble and YSU tended to handle fronts the best, and there was much variation in the worst scheme.

There was one case in particular that had unusually high errors in the NAM-initialized schemes, but not the GFS-initialized schemes for the WRF due to synoptic conditions. A warm front passed over the area during the period November 1, 2008 to November 2, 2008 and there was warm air advection occurring. The NAM accounted for this warm air advection to a much greater degree, causing a 20°C difference in temperatures between it and the GFS. This eventually resulted in a difference of about 8 m s^{-1} to 9 m s^{-1} in forecasted winds speeds (Figs. 15 & 16) and caused large errors in the NAM. Even if this date is taken out of the average MAE values, though, the GFS is still more accurate than the NAM for day 2 forecasts. The average MAE of the NAM would then be 2.014 m s^{-1} instead of 2.266 m s^{-1}, but the GFS average MAE is still over 0.3 m s^{-1} less.

5. Conclusion

With only one forecast hour, for one scheme with a MAE above 2.00 m s^{-1} (Table 2), the hypothesis is true for the GFS-initialized schemes over all cases. The hypothesis is not true for every season, though, since the upper bound of the 95% confidence interval crosses the 2.0 m s^{-1} threshold for all except spring. It is crossed by less than 0.1 m s^{-1}, though. With only four occurrences of MAE *below* 2.00 m s^{-1} (Table 3), the hypothesis is false for the NAM-initialized schemes over all cases, as well as for each season.

If the November 1, 2008 case is taken out as an anomaly, the NAM still performs worse than the GFS, but is closer to satisfying the hypothesis. The MYNN 3.0, YSU, and ensemble mean schemes for the NAM initialization would then meet the hypothesis, but the MYJ, MYNN 2.5, Pleim, and QNSE would not. So, while synoptic conditions play a role in the accuracy of the forecasts, there is still consistency in which initialization is best (GFS), which PBL schemes are best (ensemble, YSU), and which PBL schemes are worst (QNSE). Since some combinations of initializations and PBL schemes are fairly successful, there is an opportunity for wind energy companies and other interested par-

ties to improve their wind speed forecasts through the WRF.

With further analyses of the role of synoptic conditions it may become possible to create dynamic bias corrections, particularly if some schemes demonstrate unique skill under certain weather conditions or time of day. However, more research with tall tower observed data is needed to verify these results and to see how often particularly erroneous forecast cases occur.

ACKNOWLEDGEMENTS

I would like to thank Eugene Takle for his guidance throughout this project. I would also like to thank Adam Deppe for providing the model data and other assistance, MidAmerican Energy Company for providing the observed data, and members of Iowa State's "wind team" such as Bill Gallus, Chris Anderson, and Dan Rajewski for their ideas and assistance.

REFERENCES

Andersen, T. K., 2007: Climatology of surface wind speeds using a regional climate model. B.S. thesis, Dept. of Geological and Atmospheric Sciences, Iowa State University, 11 pp.

Archer, C. L., and M. Z. Jacobson, 2005: Evaluation of global wind power. *J. Geophys. Res.*, **110,** D12110.

Buckley, R. L., A. H. Weber, and J. H. Weber, 2004: Statistical comparison of Regional Atmospheric Modelling System forecasts with observations. *Meteorol. Appl.*, **11,** 67-82.

Burton, T., E. Bossanyi, N. Jenkins, and D. Sharpe, 2001: The wind resource. *Wind Energy Handbook*, John Wiley & Sons Ltd, 11-39.

Dudhia, J., cited 2009: WRF Physics. [Available online at http://www.mmm.ucar.edu/wrf/users/tutorial/200909/14_ARW_Physics_Dudhia.pdf]

Elliott, D., and M. Schwartz, 2005: Towards a wind energy climatology at advanced turbine hub-heights. Preprints, *15th Conf. on Applied Climatology*, Savannah, GA, Amer. Meteor. Soc., JP1.9.

Klink, K., 2007: Atmospheric circulation effects on wind speed variability at turbine height. *J. Appl. Meteorol. and Climatol.*, **46,** 445-456.

Pryor S. C., R. J. Barthelmie, D. T. Young, E. S. Takle, R. W. Arritt, D. Flory, W. J. Gutowski Jr., A. Nunes, J. Roads, 2009: Wind speed trends over the contiguous United States. *J. Geophys. Res.*, **114,** D14105, doi: 10.1029/2008JD011416.

Takle, E. S., J. M. Brown, and W. M. Davis, 1978: Characteristics of wind and wind energy in Iowa. *Iowa State J. Research.*, **52,** 313-339.

University Corporation for Atmospheric Research, cited 2009: Tutorial class notes and user's guide: MM5 Modeling System Version 3. [Available online at http://www.mmm.ucar.edu/mm5/documents/MM5_tut_Web_notes/MM5/mm5.htm]

Zhang, D., and W. Zheng, 2004: Diurnal cycles of surface winds and temperatures as simulated by five boundary layer parameterizations. *J. Appl. Meteorol.*, **43,** 157-169.

APPENDIX

Abbreviation	Planetary Boundary Layer Scheme	Description of Main Features
Blackadar	High-resolution Blackadar PBL	Suitable for high resolution PBL. Uses four stability regimes and split time steps for stability.
MYJ	Mellor-Yamada-Janjic	Eta operational scheme. One-dimensional prognostic turbulent kinetic energy scheme with local vertical mixing
MYNN 2.5	Mellor-Yamada-Nakanishi and Niino Level 2.5 PBL	Predicts sub-grid TKE terms. New in Version 3.1.
MYNN 3.0	Mellor-Yamada-Nakanishi and Niino Level 3 PBL	Predicts TKE and other second-moment terms. New in Version 3.1.
Pleim	ACM2 PBL or Pleim	Asymmetric Convective Model with non-local upward mixing and local downward mixing
QNSE	Quasi-Normal Scale Elimination PBL	A TKE-prediction option that uses a new theory for stably stratified regions. New in Version 3.1.
YSU	Yonsei University Scheme	Non-local-K scheme with explicit entrainment layer and parabolic K profile in unstable mixed layer

Table 1: Planetary boundary layer schemes with abbreviations and descriptions of main features

Hour	MYJ GFS	MYNN 2.5 GFS	MYNN 3.0 GFS	Pleim GFS	QNSE GFS	YSU GFS	Ensemble GFS
38	1.872	1.874	1.711	2.103	1.820	1.440	1.576
39	1.630	1.720	1.587	1.765	1.573	1.550	1.492
40	1.318	1.444	1.393	1.548	1.463	1.568	1.327
41	1.622	1.733	1.702	1.730	1.755	1.602	1.501
42	1.744	1.752	1.778	1.790	1.737	1.575	1.599
43	1.828	1.830	1.854	1.649	1.940	1.652	1.631
44	1.753	1.798	1.726	1.764	1.748	1.581	1.575
45	1.979	1.828	1.791	1.786	1.946	1.727	1.726
46	1.865	1.752	1.778	1.619	1.805	1.849	1.669
47	1.754	1.772	1.717	1.576	1.805	1.505	1.498
48	1.581	1.686	1.588	1.389	1.721	1.115	1.230
AVG	1.723	1.744	1.693	1.702	1.756	1.560	1.529

Table 2: Mean absolute error ($m\ s^{-1}$) for day 2 of WRF – GFS forecasts with average

Hour	MYJ NAM	MYNN 2.5 NAM	MYNN 3.0 NAM	Pleim NAM	QNSE NAM	YSU NAM	Ensemble NAM
38	1.838	2.102	2.066	2.471	2.110	2.113	1.740
39	1.864	2.163	2.059	2.381	2.192	2.087	1.887
40	2.414	2.256	2.216	2.513	2.428	2.237	2.132
41	2.376	2.427	2.373	2.378	2.535	2.349	2.212
42	2.639	2.837	2.810	2.621	2.787	2.442	2.580
43	2.734	2.699	2.744	2.916	2.725	2.535	2.544
44	2.479	2.618	2.463	2.474	2.694	2.255	2.364
45	2.191	2.240	2.129	2.208	2.497	2.245	2.125
46	2.165	1.952	1.953	2.089	2.125	2.063	1.943
47	2.267	2.170	2.169	1.943	2.416	2.077	1.989
48	1.933	1.835	1.845	1.682	2.121	1.699	1.563
AVG	2.264	2.300	2.257	2.334	2.421	2.191	2.098

Table 3: Mean absolute error (m s^{-1}) for day 2 of WRF – NAM forecasts with average

Season	Lower 95% CI Bound	Mean MAE	Upper 95% CI Bound
Winter	1.500	1.797	2.094
Spring	1.135	1.401	1.667
Summer	1.587	1.810	2.034
Fall	1.498	1.796	2.094

A

Season	Lower 95% CI Bound	Mean MAE	Upper 95% CI Bound
Winter	2.167	2.377	2.586
Spring	1.250	1.555	1.860
Summer	2.032	2.553	3.073
Fall	2.481	2.719	2.957

B

Table 4: Average mean absolute error (m s^{-1}) with a 95% confidence interval for the day 2 daytime forecast period for each season initialized by A) GFS and B) NAM

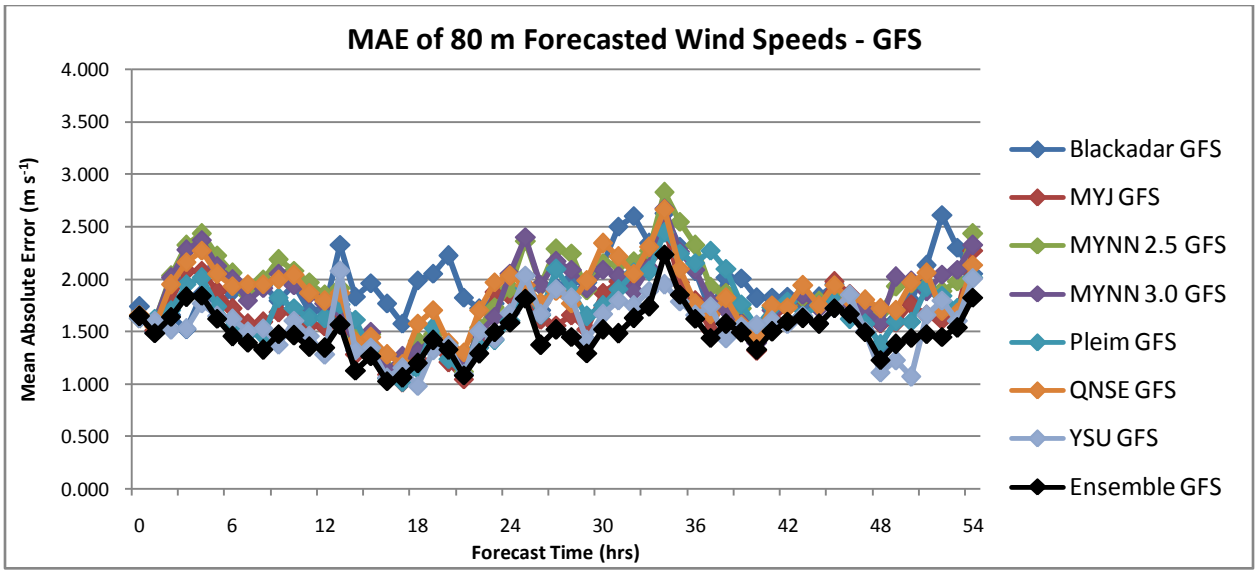

Figure 3: Mean absolute error of GFS forecasts through entire forecast period

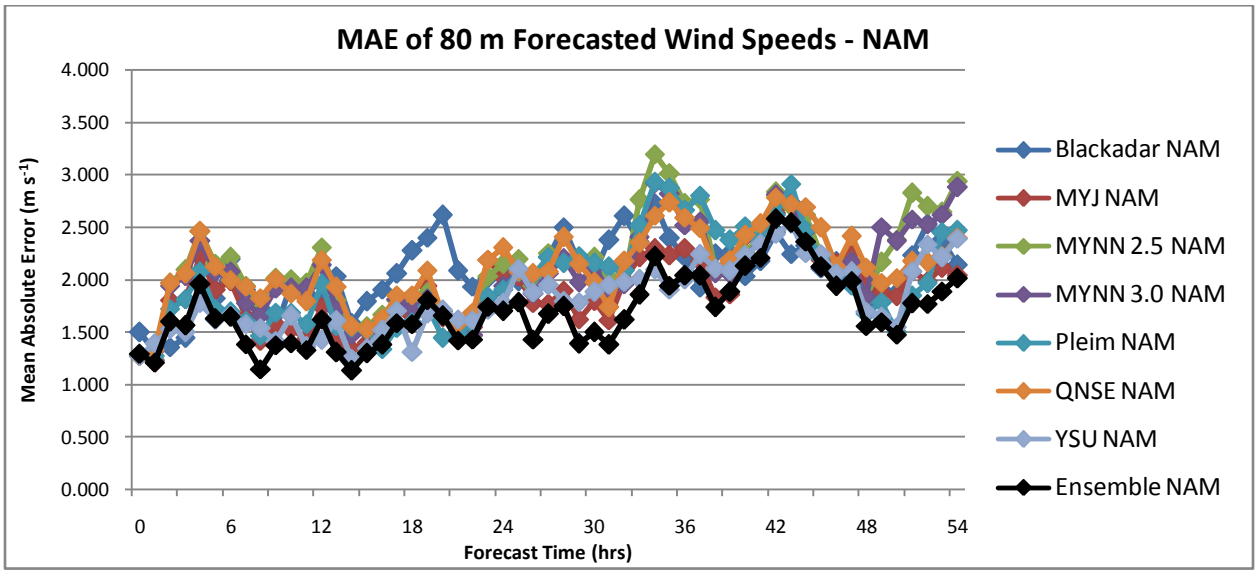

Figure 4: Mean absolute error of NAM forecasts through entire forecast period

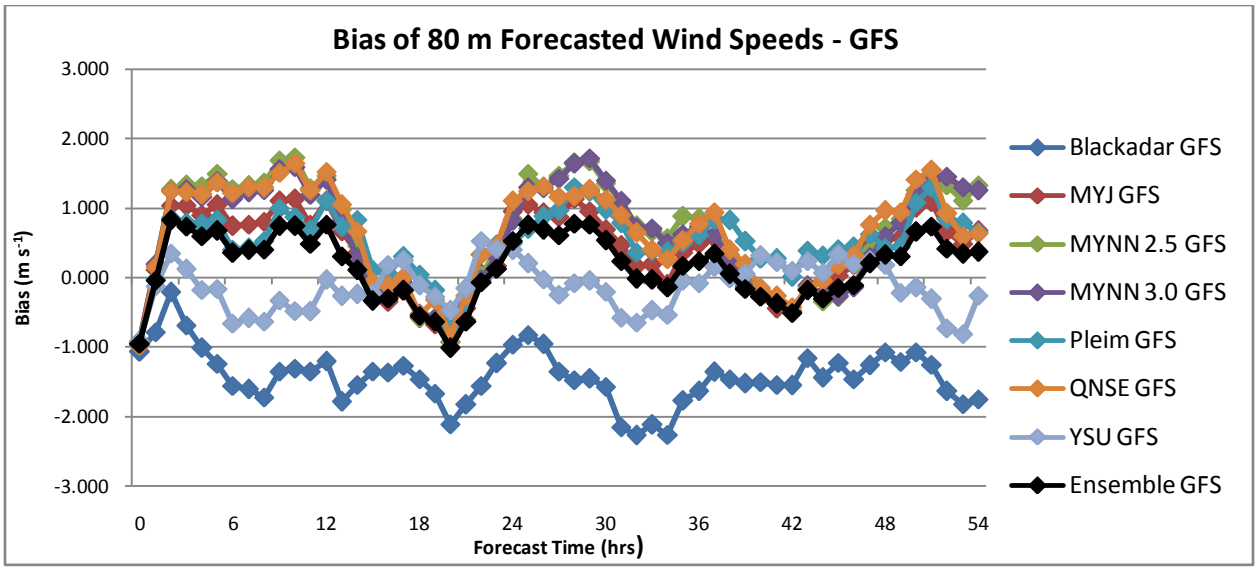

Figure 5: Bias of GFS forecasts through entire forecast period

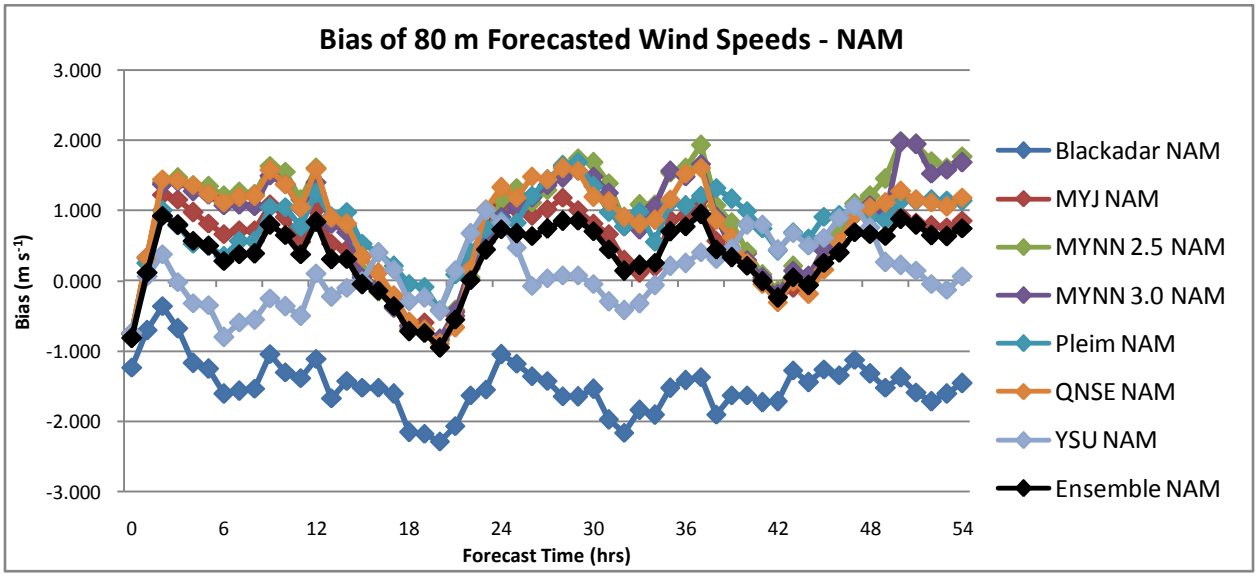

Figure 6: Bias of NAM forecasts through entire forecast period

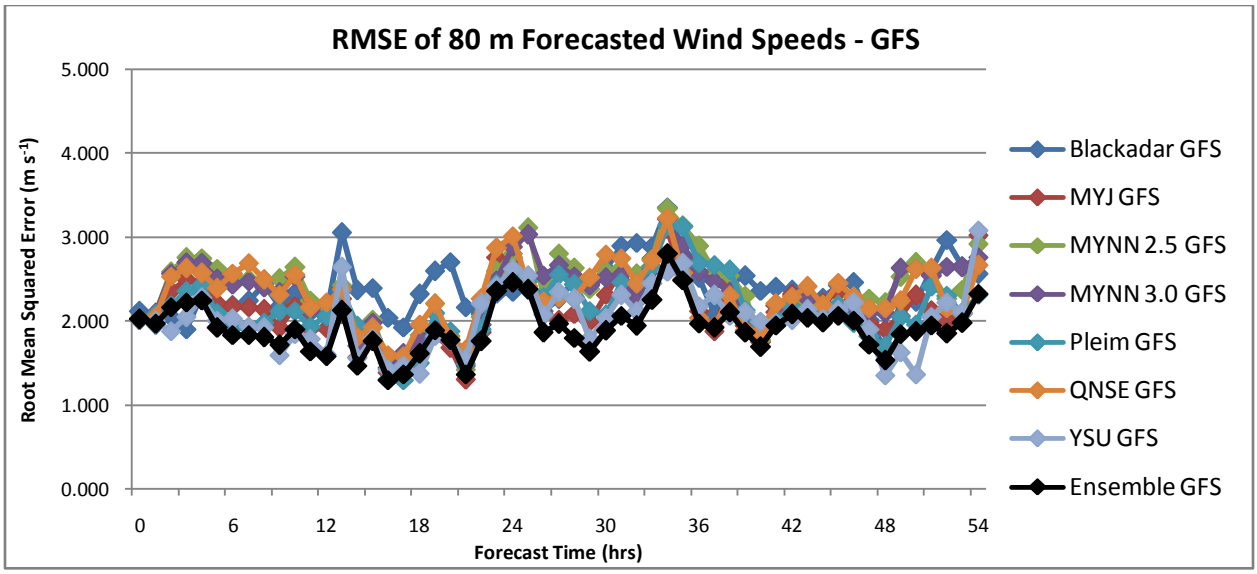

Figure 7: Root mean squared error of GFS forecasts through entire forecast period

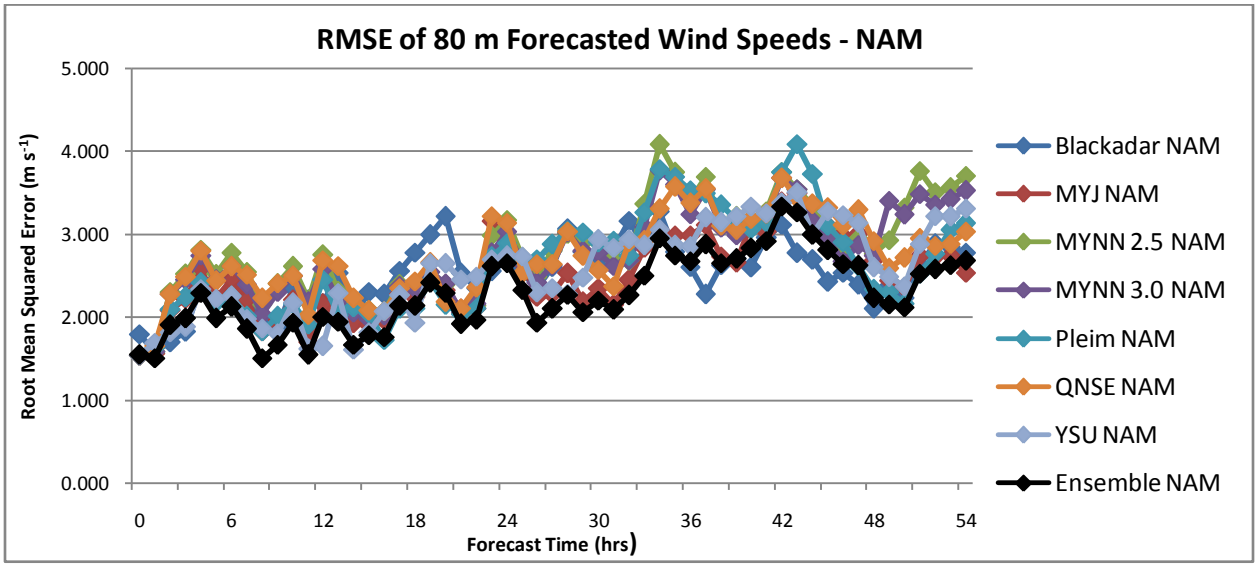

Figure 8: Root mean squared error of NAM forecasts through entire forecast period

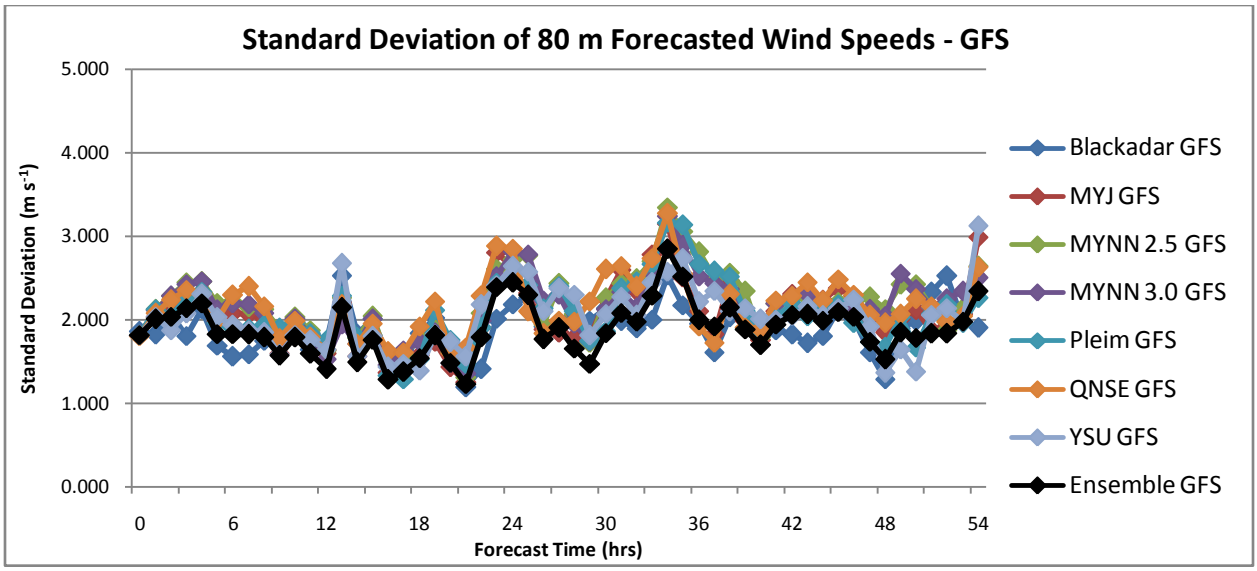

Figure 9: Standard deviation of GFS forecasts through entire forecast period

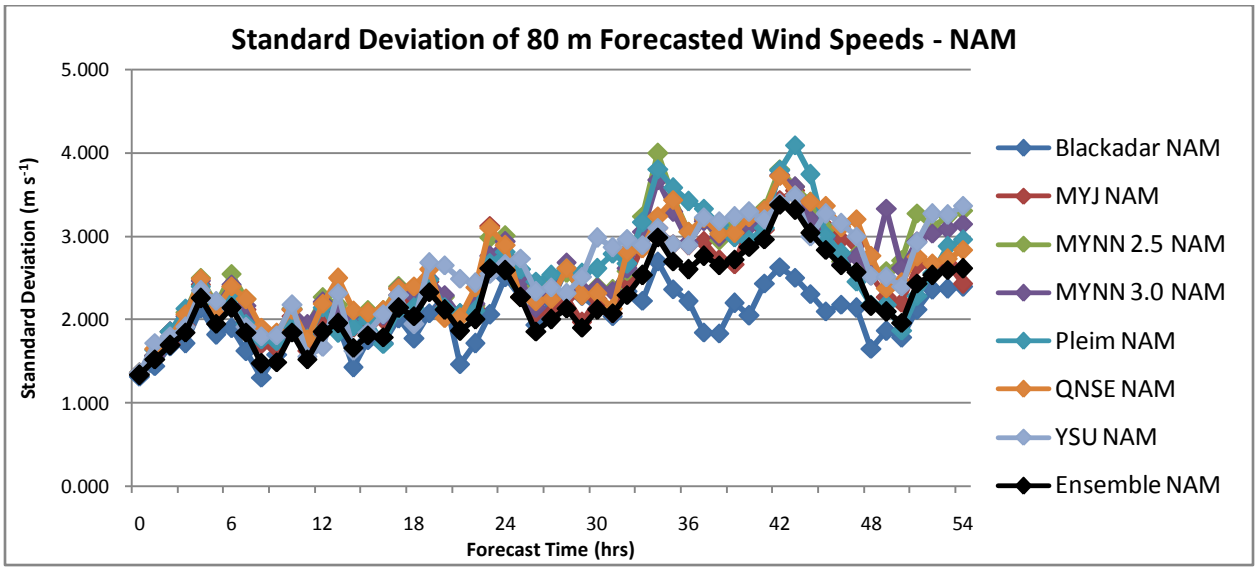

Figure 10: Standard deviation of NAM forecasts through entire forecast period

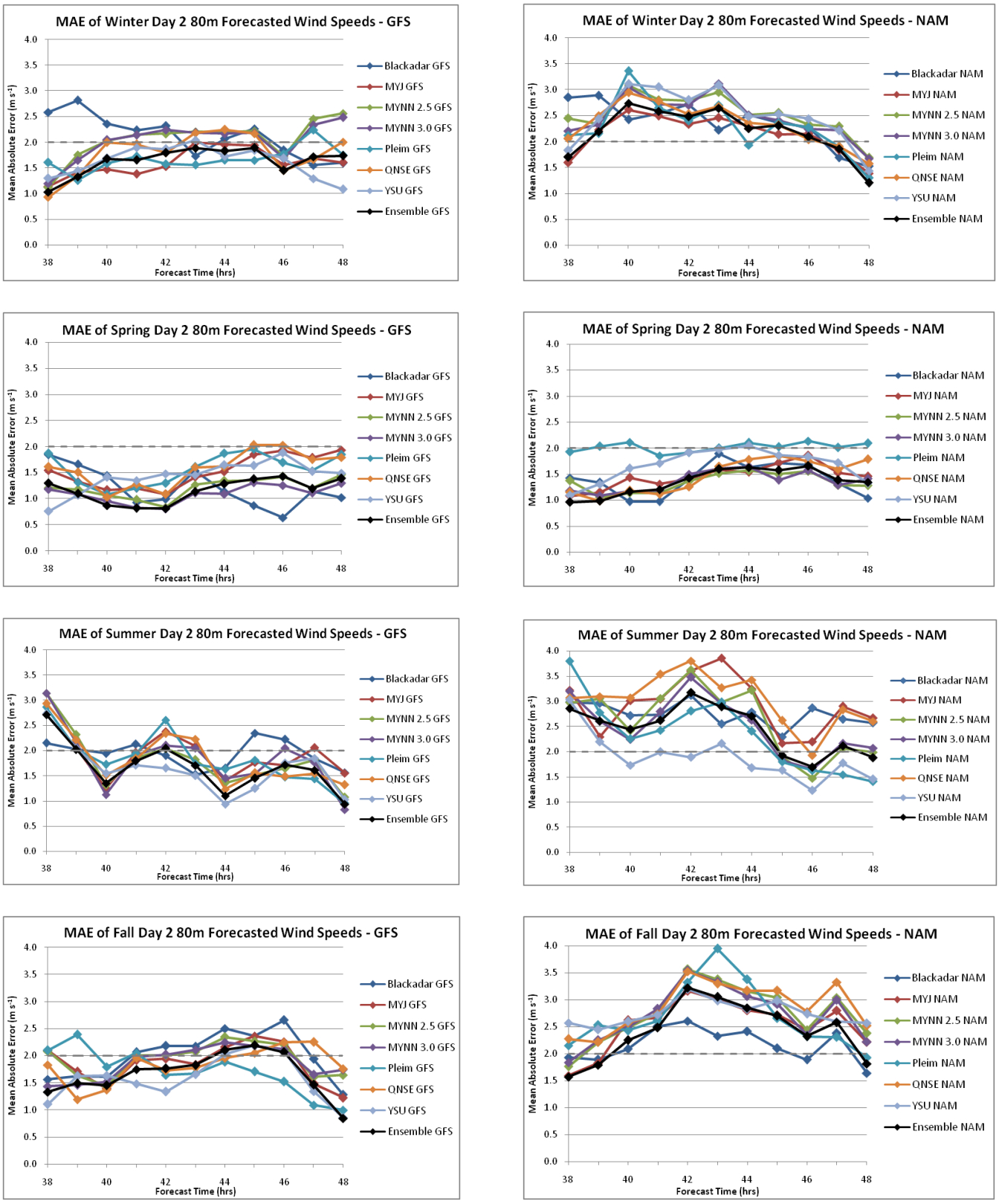

Figure 13: Mean absolute error of daytime day 2 wind speeds for GFS and NAM initializations, respectively, and for winter, spring, summer, and fall seasons, respectively

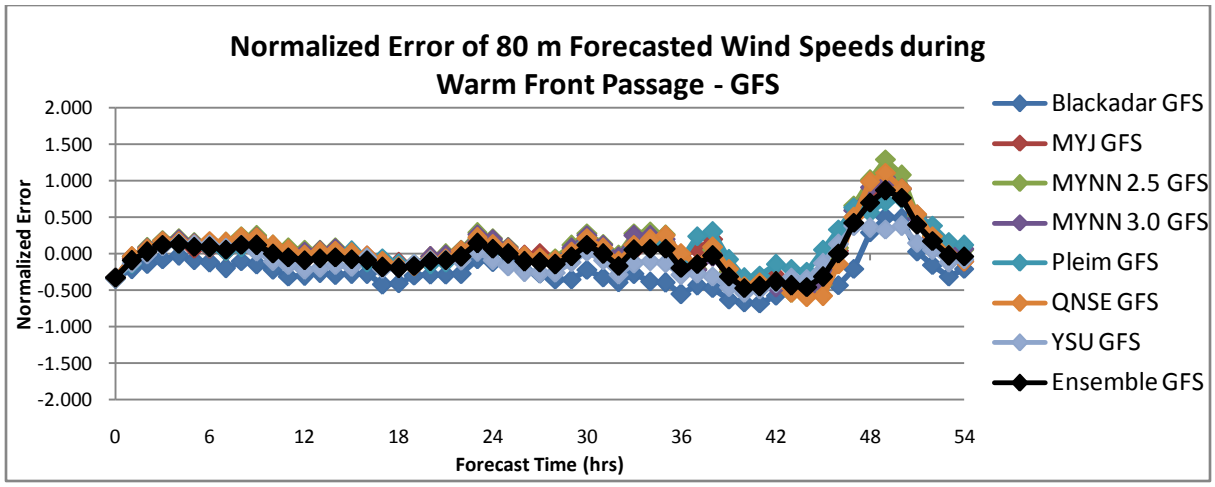

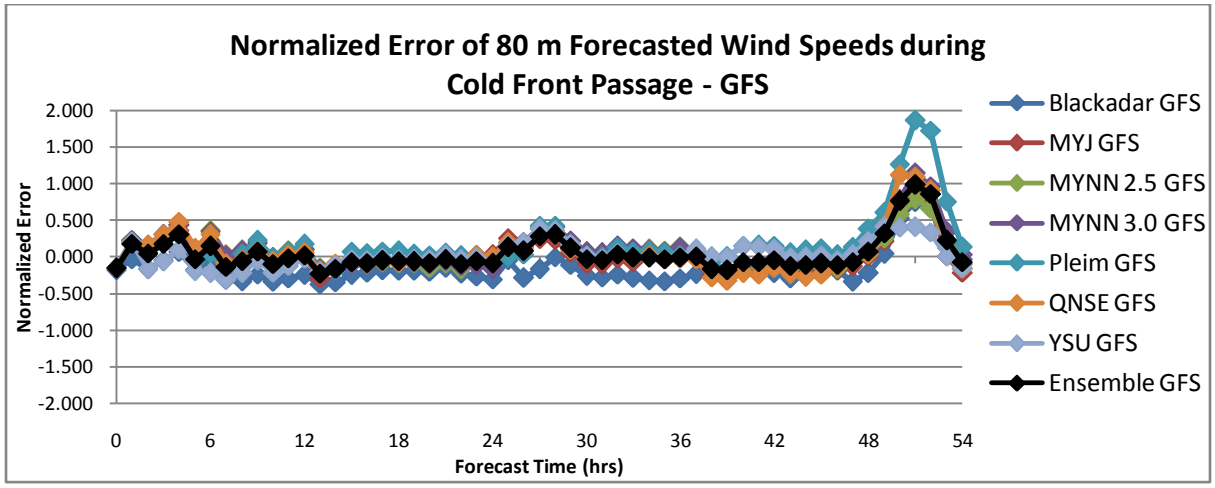

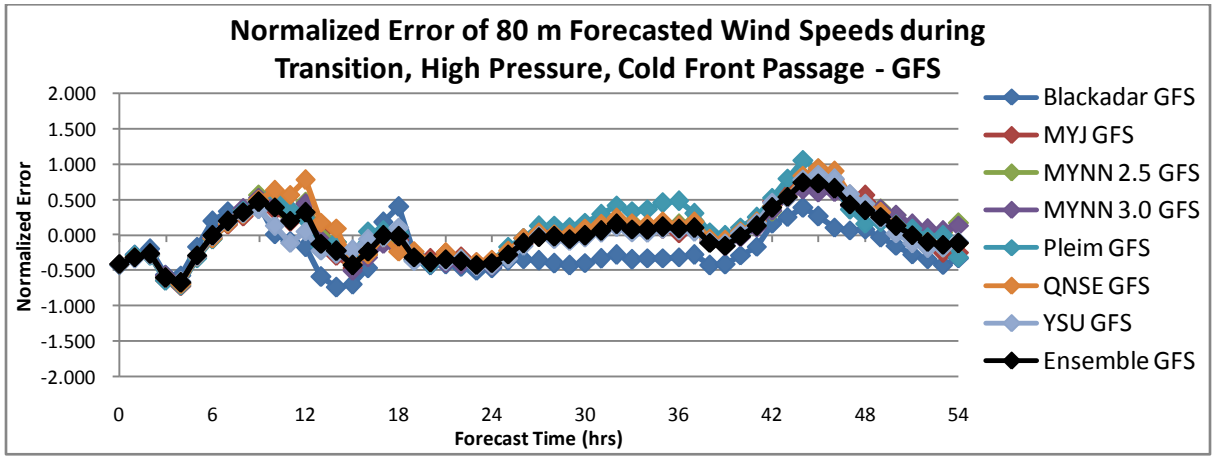

Figure 14: Normalized error of GFS forecasted wind speeds during changes in synoptic conditions (NAM results were similar in nature)

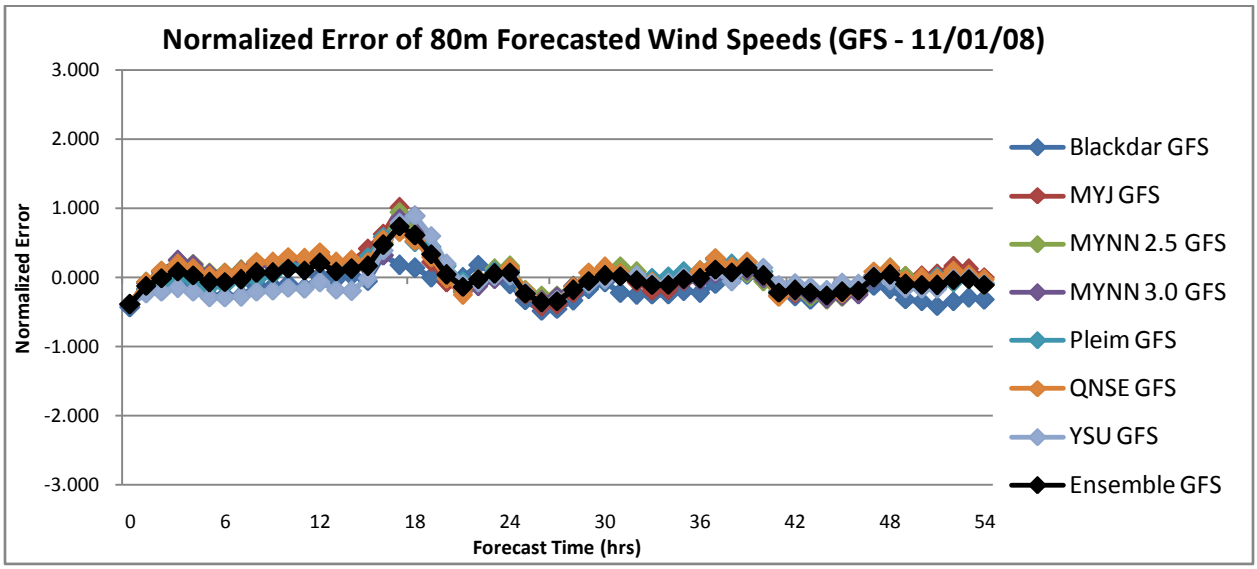

Figure 15: Normalized error of GFS forecasts for 11/01/2008

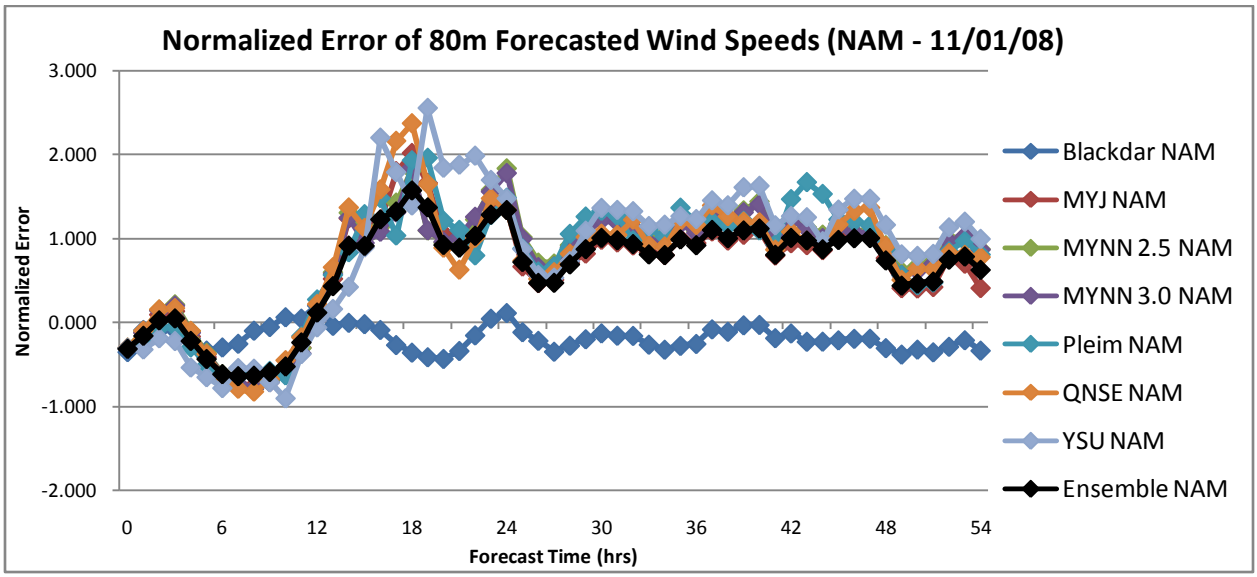

Figure 16: Normalized error of NAM forecasts for 11/01/2008